Journal of NeuroVirology, 12: 116–128, 2006

ISSN: 1355-0284 print / 1538-2443 online
DOI: 10.1080/13550280600716604

Taylor & Francis
Taylor & Francis Group

Characterization of lymphocytic infiltrates in progressive multifocal leukoencephalopathy: Co-localization of CD8$^+$ T cells with JCV-infected glial cells

Christian Wüthrich,[1] Santosh Kesari,[2,3] Woong-Ki Kim,[1] Kenneth Williams,[1] Rebecca Gelman,[3] Derek Elmeric,[3] Umberto De Girolami,[2] Jeffrey T Joseph,[4] Tessa Hedley-Whyte,[5] and Igor J Koralnik[1,4]

[1]Division of Viral Pathogenesis and [4]Department of Neurology, Beth Israel Deaconess Medical Center, Boston, Massachusetts, USA; [2]Departments of Pathology, Brigham and Women's Hospital and Children Hospital, Boston, Massachusetts, USA; [3]Dana Farber Cancer Institute and Harvard School of Public Health, Boston, Massachusetts, USA; [5]Department of Pathology, Massachusetts General Hospital, Harvard Medical School, Boston, Massachusetts, USA

We characterized inflammatory infiltrates in archival brain biopsy and autopsy samples from 26 HIV$^+$ and 20 HIV$^-$ patients with progressive multifocal leukoencephalopathy (PML). The predominant inflammatory cells were CD8$^+$ T lymphocytes. We defined CD8$^+$ T cell distribution with regard to JCV-infected glial cells, PML lesions and the extent of demyelination. In most samples from either HIV$^+$ and HIV$^-$ patients, we found positive correlations between the parenchymal CD8$^+$ T cells and JCV-infected glial cells and conversely, negative correlations between the perivascular CD8$^+$ T cells and JCV-infected glial cells in the surrounding brain. Most of these correlations remained significant after accounting for the degree of demyelination and location of the cells relative to lesions. Moreover, high numbers of CD8$^+$ T cells were found within and at the border of active PML lesions. These results suggest that CD8$^+$ T cells are primarily associated with JCV-infected glial cells in most PML cases and that an active ongoing recruitment of CD8$^+$ T cells and possibly viral antigen-specific retention could occur. These observations are discussed in the context of the recent evidence of PML in multiple sclerosis and Crohn's patients treated with natalizumab, underscoring the role of CD8$^+$ T lymphocytes in continued immunosurveillance of the CNS. *Journal of NeuroVirology* (2006) **12,** 116–128.

Keywords: CNS; demyelination; HIV; immune response; PML

Introduction

Progressive multifocal leukoencephalopathy (PML) (Astrom *et al*, 1958) is a deadly opportunistic infection of the central nervous system (CNS), caused by the polyomavirus JC (JCV) (Padgett *et al*, 1971). Anti-JCV antibodies are present in approximately 85% of healthy adults. Primary infection with JCV is asymptomatic, but its reactivation in the setting of immunosuppression can induce a lytic infection of oligodendrocytes. Although it was initially described as a rare infection in patients with chronic lymphocytic leukemia (CLL), lymphomas or organ transplant

Address correspondence to Igor J. Koralnik, MD, Department of Neurology, Beth Israel Deaconess Medical Center, Research East, 213 C, 330 Brookline Avenue, Boston, MA 02215, USA. E-mail: ikoralni@bidmc.harvard.edu

This work was supported in part by NIH grant R01 NS041198 and 047029 to IJK, NS037654 and 040237 to KW, and P30 AI28691 (Harvard CFAR), which supported RG, and the Ellen R. Cavallo research fund.

We are grateful to Dr Susan Morgello and Benjamin B. Gelman for providing PML samples through the National NeuroAIDS tissue consortium, including the Manhattan HIV Brain Bank (R24MH59724) and the Texas Repository for AIDS Research (R24NS045491). We are thankful to Brice Due for technical assistance.

Received 26 December 2005; accepted 23 March 2006.

recipients, patients with AIDS now account for more than 80% of all PML cases (Koralnik *et al*, 2004). There is no treatment for JCV and the prognosis of PML is poor. At the beginning of the HIV epidemic, only 9% of AIDS patients with this disease survived more than a year (Berger *et al*, 1998). Since the introduction of highly active antiretroviral therapy (HAART), this number has increased to approximately 50% (Antinori *et al*, 2003).

The histopathological characteristics of brains of patients with PML include single or multiple areas of demyelination containing: a) JCV-infected oligodendrocytes with enlarged amphophilic nuclei located at the periphery of the lesions; b) reactive gliosis, with enlarged, bizarre astrocytes, some sustaining a restrictive, non-lytic JCV infection and c) an inflammatory response largely composed of lipid-laden macrophages phagocytosing myelin and cellular debris. Despite the abundance of JC virions in PML lesions, a lymphocytic infiltrate has been shown in only one study in HIV-infected patients (Aksamit *et al*, 1990). It is unclear whether these cells represent only a coincident response to HIV, rather than to JCV. Furthermore, the composition of these infiltrates has not been studied in detail. Better knowledge of the immune response that is active within lesions of PML is urgently needed in light of the recent development of PML in two patients with multiple sclerosis (MS) and one with Crohn's disease treated with natalizumab, a novel immunomodulatory medication which prevents migration of lymphocytes and monocytes in the brain parenchyma (Berger and Koralnik, 2005; Drazen, 2005; Kleinschmidt-Demasters and Tyler, 2005; Langer-Gould *et al*, 2005; Van Assche *et al*, 2005).

The authors have explored the cellular immune response in PML in blood, and have characterized JCV-specific CD8$^+$ cytotoxic T lymphocytes (CTL) (Du Pasquier *et al*, 2003; Koralnik *et al*, 2002; Koralnik *et al*, 2001). They have shown that these CTL play a crucial role in the containment of JCV early in disease, and that their presence is associated with prolonged survival and a more favorable clinical outcome (Du Pasquier *et al*, 2004). Whether such JCV-specific CD8$^+$ T cells can also be found in the CNS of PML patients and function to control virus is unknown. This is due in part to the inability to use JCV MHC class I tetrameric complexes to identify JCV specific CD8$^+$ T cells in formalin fixed or frozen pathology tissues. In addition, until recently, direct staining of CD8$^+$ T cells in formalin-fixed, paraffin-embedded samples has also been technically challenging (Kim *et al*, 2004) although rare PML cases have been reported with substantial inflammatory infiltrates and a more protracted clinical course (Richardson and Johnson, 1975).

Using a multi-layer image analysis, we found a predominance of CD8$^+$ T cells adjacent to and within PML lesions. Furthermore, we found a significant association of CD8$^+$ T cells with JCV-infected cells in the brain parenchyma in HIV$^+$ and HIV$^-$ individuals with PML. Lastly, in active PML lesions we found CD8$^+$ T cells on the lesion border. These results suggest that these cells not only are on the active edge of the lesion with JCV-infected cells, but that they may possibly also contribute to containment of disease progression.

Results

Characterization of inflammatory infiltrates in PML lesions

We studied the phenotype of inflammatory cells in PML lesions in 31 PML cases from 25 HIV$^+$ and 6 HIV$^-$ patients. In HIV$^+$ patients and HIV$^-$ patients without CLL, lymphocytic infiltrates in PML lesions (Figure 1A and B) were predominantly CD3$^+$ T cells (99% of cells) (Figure 1C and D), whereas CD20$^+$ B cells were only rarely seen (<0.1% of cells, data not shown). IHC performed on serial sections showed that the majority of CD3$^+$ T cells (99%) were also CD8$^+$ (Figure 1C and D), whereas CD4$^+$ T cells were absent or infrequent (<0.1% of cells, data not shown), similar to our observations in SIV-infected animals (Kim *et al*, 2004). For this reason, subsequent quantitative analysis was performed only on CD8$^+$ T cells and JCV-infected cells.

Three HIV$^-$ PML patients with CLL had large perivascular cuffs of inflammatory cells (Figure 2A). Double and triple IHC experiments showed that 75–99% of these cells were CD20$^+$ B cells (Figure 2B and D), consistent with the patient's leukemia, while the other lymphocytes were CD8$^+$ T cells (Figure 2C). In the parenchyma of the same patients, CD20$^+$ B cells accounted for less than 1% of the total lymphocytes (Figure 2B and D), and the main lymphocyte population were CD8$^+$ T cells (Figure 2C). Double IHC experiments showed that all JCV-infected cells (blue staining in Figure 2B–D) were in the parenchyma, and none were in perivascular cuffs.

In 25 HIV$^+$ patients with PML, the proportion of CD20$^+$ B cells located in small perivascular cuffs was less than 10% in 4 cases, less than 1% in 6 cases and absent in the 15 remaining cases. In the parenchyma, CD20$^+$ B cells accounted for less than 1% of lymphocytes. These results demonstrated that CD8$^+$ T cells are the major lymphocyte subsets in the brain lesions of both HIV$^+$ and HIV$^-$individuals with PML.

Quantitative observations

Having determined that CD8$^+$ T cells are the major inflammatory cell type in PML lesions, we sought to characterize their topographic localization with regard to JCV-infected cells to study the possibility that such cells have trafficked to and remained in the CNS, perhaps in an antigen-specific manner. Since it is not possible to use MHC class I tetramers in fixed tissue to obtain direct evidence of the specificity of CD8$^+$ T cells for JCV, we used the proximity of

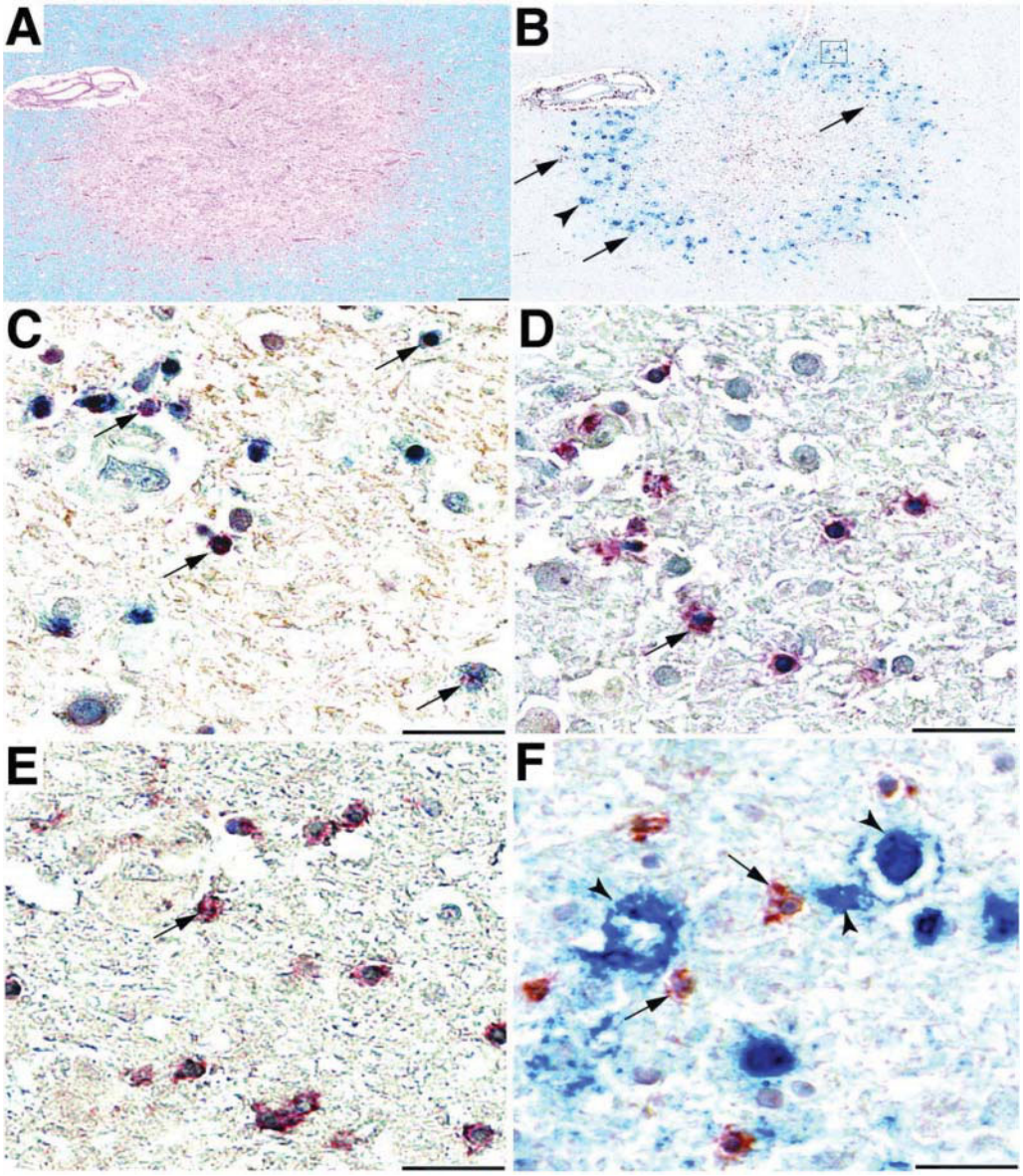

Figure 1 $CD8^+$ T cells are the main lymphocyte cell type in the PML lesions of an HIV^+ individual. A single demyelinated lesion can be seen with hematoxylin and eosin (H&E) stain and Luxol Fast blue (LFB) (Panel A, bar: 100 μm). In panel B, double staining with anti CD8 ab and anti polyomavirus ab (with hemotoxylin counterstainig of nuclei) reveals numerous $CD8^+$ cells (brown cells with purple nuclei, arrows) around JCV-infected cells (blue nuclear and/or cytoplasmic staining, arrowheads; bar: 100 μm). The box shows the area studied at high magnification on contiguous slides in panels C-F. The results of double staining experiment with anti CD3 (purple) and CD8 abs (blue) indicate that most $CD3^+$ cells were also $CD8^+$ (purple cells with variable amount of blue overlay, arrows) (Panel C; bar 10 μm). Single staining experiment with anti CD3 Ab (purple cells with blue, hematoxylin counterstained nuclei, arrows) (Panel D, bar: 10 μm) and anti CD8 Ab (purple cells with blue, hematoxylin counterstained nuclei, arrows) (Panel E, bar: 10 μm) showed similar results in cell frequencies and location. The proximity of $CD8^+$ T cells (brown cells with purple nuclei, arrows) and JCV-infected cells (blue nuclear and/or cytoplasmic staining, arrowheads) is shown in Panel F (bar: 10 μm).

$CD8^+$ T cells to JCV-infected cells as indirect, correlative evidence of their antigenic specificity. For this, we devised a multi-layer image analysis (Figure 3).

Patients and specimen characteristics used for quantitative observations are shown in Table 1. We first compared $CD8^+$ T cells within the CNS of PML patients and controls taking into account both parenchymal and vessel-associated $CD8^+$ T cells. The median densities of $CD8^+$ T cells in the control autopsy specimens from patients with PML were more than 10 times the median densities of the $CD8^+$ T cells in the autopsy specimens without PML ($p = 0.0006$, Table 2). This highly significant difference was primarily due to a lower density of $CD8^+$ T cells in the parenchyma in the controls ($p = 0.0004$, Table 2) rather than a lower density of vessel-associated

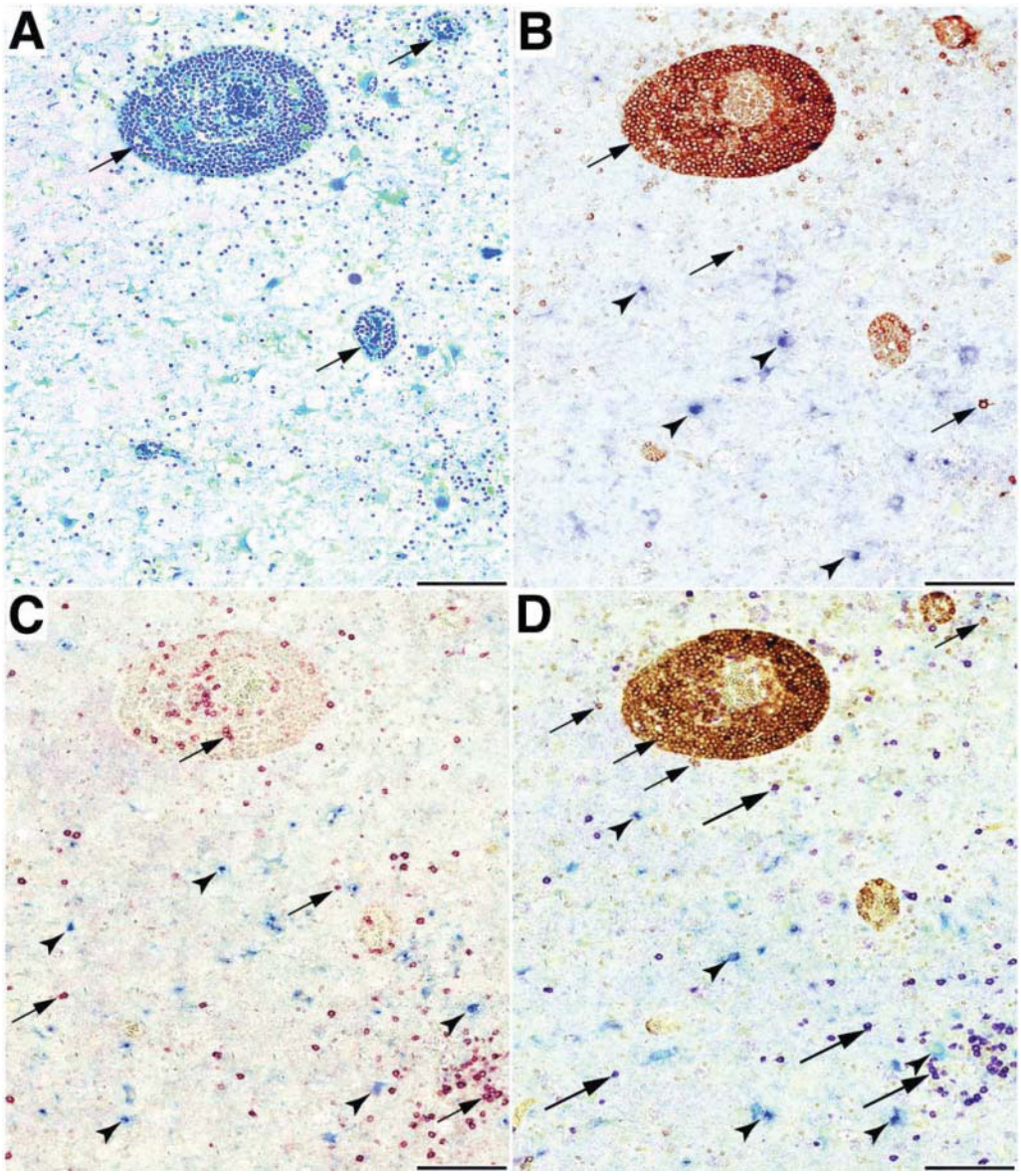

Figure 2 CD20$^+$ B cells are located in perivascular cuffs and CD8$^+$ T cells in PML lesions of an HIV$^-$ patient with CLL. A demyelinated area containing some vessels surrounded by perivascular cuffs (arrows) can be seen with H&E stain and Luxol Fast blue (LFB) (Panel A, bar: 100 μm). In panel B, double staining experiment with anti CD20 Ab and anti polyomavirus antibody reveals that most CD20$^+$ B cells (brown, arrows) are located in the perivascular cuffs, and that only a few are present in the parenchyma (blue, arrowheads) (bar: 100 μm). Conversely CD8$^+$ T cells (purple, arrows) are more rare in the perivascular cuffs, but can be seen in higher numbers in the parenchyma, where most JCV-infected cells (blue, arrowheads) are also located (panel C, bar: 100 μm). In panel D (bar: 100 μm) triple staining experiment allows concomitant visualization of perivascular CD20$^+$B cells (brown, short arrows), parenchymatous CD8$^+$ T cells (purple, long arrows) and JCV-infected glial cells (blue, arrowheads).

CD8$^+$ T cells ($p = 0.04$, Table 2). The control autopsy specimens are omitted from the rest of these analyses.

The median density of the CD8$^+$ T cells in the biopsies, from both HIV$^-$ and HIV$^+$ PML patients, was about 2 times higher than the autopsies (Table 2), mainly because the squares with no JCV-infected cells and no CD8$^+$ T cells were included in the frequency calculation and all the autopsies but only some of the biopsies contained grid squares with zero CD8$^+$ T cells ($p = 0.0001$). Among the autopsies, there was no significant difference between HIV$^+$ and HIV$^-$ PML patients in CD8$^+$ T cell densities ($p = 0.77$, Table 2). The biopsies from HIV$^+$ PML patients had larger CD8$^+$ T cell densities than the biopsies from HIV$^-$ PML patients, which did not reach statistical significance ($p = 0.06$, Table 2).

We then examined the densities of JCV-infected cells and CD8$^+$ T cells in the parenchyma of the autopsy specimens according to their location in the PML lesions and to the degree of demyelination. We

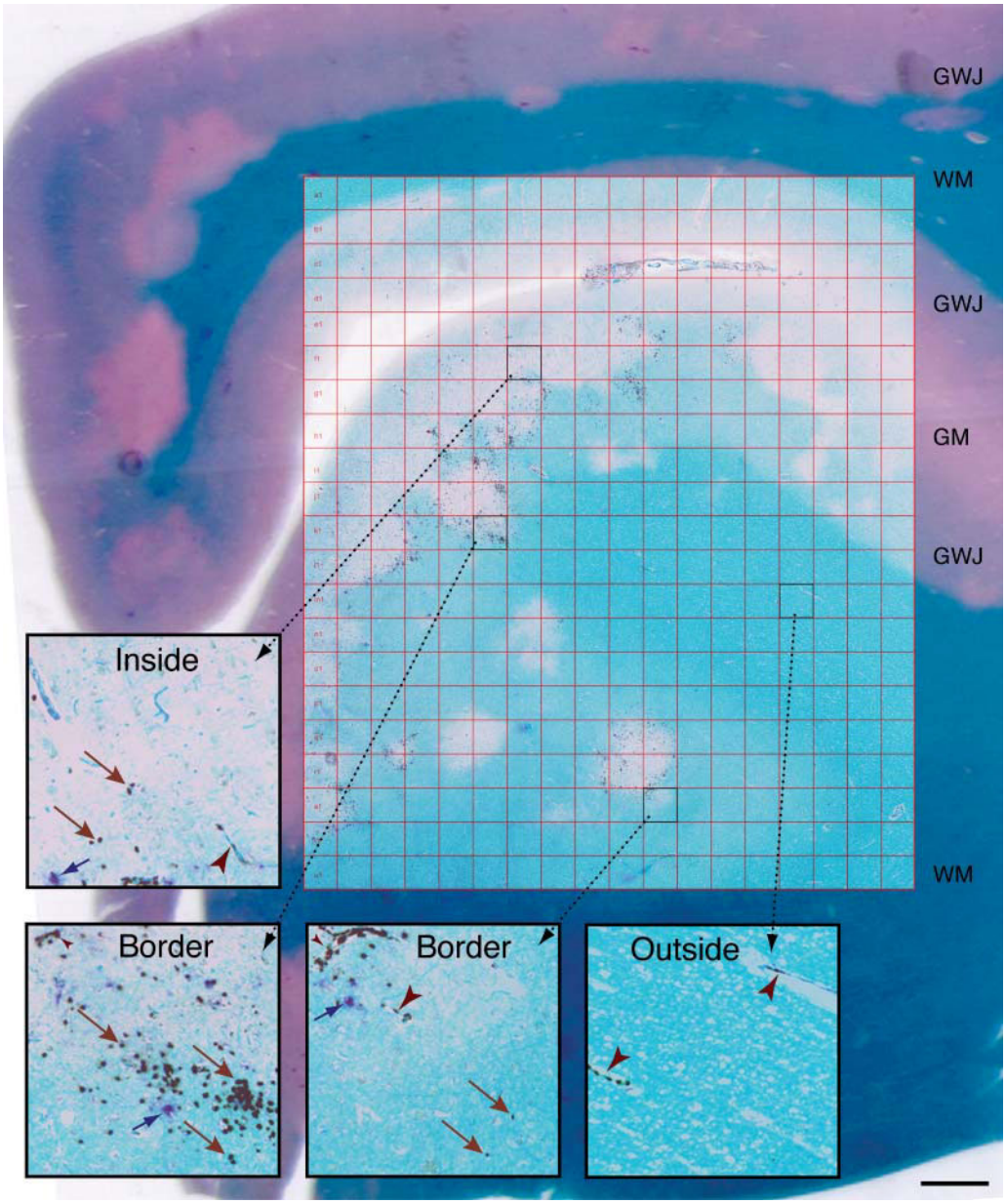

Figure 3 Multi-layer topographic mapping of JCV-infected cells and CD8+ T cells in an HIV+ individual with PML. First layer: low resolution image (1200 dpi scan) from a section stained with luxol fast blue (LFB) and hematoxylin and eosin (H&E) showing the architecture of the tissue and the extent of demyelination. Second layer: high resolution (1.185 pix/μm) montage of approximately 300 contiguous pictures spanning an entire slide stained by IHC for polyomavirus Ab and CD8 and counterstained with LFB, showing the distribution of the JCV-infected and CD8+ T cells of the sampled area. Third layer: 600 × 600 μm (711 × 711 pixels) square grid covering the sampled area. Characteristic samples of squares localized inside, at the border, or outside of the areas of demyelination are showed as insets; Blue arrows, JCV-infected cells; brown-red arrowheads, CD8+ T cells associated with blood vessels; brown-red arrows, CD8+ T cells located in the parenchyma. GWJ, Gray-white junction; WM, white matter; GM, gray matter (bar: 1 mm).

found that the density of both cell types tended to increase going towards the lesions (Figure 4). In areas of low demyelination, the densities of CD8+ T cells and JCV-infected cells were slightly higher in the squares that are less than 1.8 mm distant from the PML lesions compared with the squares that are more than 1.8 mm distant from the lesions and the densities of CD8+ T cells and JCV-infected cells were significantly higher in the squares at the border of the lesions compared with the squares that are less than 1.8 mm distant from the PML lesions. (A 1.8 mm distance is the length of 3 grid squares). However in areas of high demyelination there was no difference in the CD8+ T cell densities at the border and inside of PML lesions and there was a non-significantly lower density of JCV-infected cells inside compared with the border of PML lesions. Finally, at the border of the PML lesions, the density of CD8+ T cells

Table 1 Patient and specimen characteristics

	All specimens		*Autopsies*		*Biopsies*	
	N	*Percent*	*N*	*Percent*	*N*	*Percent*
All	46	100	30	100	16	100
Specimen type						
Autopsy	30	65	30	100	—	—
Biopsy	16	35	—	—	16	100
HIV						
Negative	20	43	9	30	11	69
Positive	26	57	21	70	5	31
Disease						
Active	37	80	24	80	13	81
Inactive	5	11	3	10	2	13
Incidental	2	4	2	7	0	0
Unknown	2	4	1	3	1	6
Sex						
Male	29	63	20	67	9	56
Female	9	20	3	10	6	38
Unknown	8	17	7	23	1	6
Age						
30–39	10	22	8	27	2	13
40–49	12	26	8	27	4	25
50–59	6	13	3	10	3	18
60–79	7	15	2	7	5	31
Unknown	11	24	9	30	2	13
Race						
White	10	22	7	23	3	19
Black	9	20	8	27	1	6
Hispanic	1	2	1	3	0	0
Unknown	26	57	14	47	12	75
JCV staining method						
In situ hybridization	18	39	17	57	1	6
Immunohistochemistry	28	61	13	43	15	94

was significantly greater ($p = 0.03$) and the density of JCV-infected cells was not significantly greater in the squares located in highly demyelinated areas than in the squares located in low demyelination areas (data not shown in Figure 4).

Topographical relationship of CD8$^+$ T cells and JCV-infected cells

We then examined whether CD8$^+$ T cells co-localized with JCV-infected cells in the PML lesions. Table 3 summarizes, within each patient the Spearman rank correlation coefficients of the number of JCV-infected cells and CD8$^+$ T cells. This analysis was performed in each grid square with at least one CD8$^+$ T cell or one JCV-infected cell. Positive correlations between JCV-infected cells and CD8$^+$ T cells (total or parenchymal CD8$^+$ T cells in autopsies) were found in 80-83% of the patients (Table 3). They were significantly positive in 76% or more of the autopsy specimens. Positive correlations between JCV-infected cells and CD8$^+$ T cells were present in 75% of biopsies but the number of grid squares in the samples were not large enough to have reasonable power for the significance test (Table 3).

Conversely, when perivascular CD8$^+$ T cells were considered, negative correlations were found between these CD8$^+$ T cells and JCV-infected cells in the surrounding parenchyma in 76% of autopsy samples (Table 3), a significant difference compared to the mostly positive correlations between JCV-infected cells and parenchymal CD8$^+$ T cells ($p < 0.0001$). There were no significant differences between HIV$^+$ and HIV$^-$ patients regardless of sample type and location (Table 3).

We then explored whether patient characteristics influenced the correlation of CD8$^+$ T cells with JCV-infected cells. We used this correlation as the dependent variable in stepwise linear regressions using as covariates patient characteristics listed in Table 1. None of these covariates had a significant effect on these correlations, and there was adequate power for reasonable differences associated with HIV serostatus or type of specimen (autopsy vs biopsy).

It could be argued (from data such as that shown in Figure 4) that the positive correlations of CD8$^+$ T cells and JCV-infected cells are artificially large and caused by the fact that some locations in the brain tend to have more of both cell types. To verify that the correlations were due to a true co-localization of CD8$^+$ T cells with JCV-infected cells, and not to an effect of location and/or demyelination, a Poisson regression for parenchymal CD8$^+$ T cells was done treating the number of JCV- infected cells in a grid square, the location and the demyelination of the grid square all as possible explanations for the number of CD8$^+$ T cells in the square. In this model, 83% (19/23) of the specimens with significantly positive Spearman rank correlations had a significantly ($p < 0.05$) positive relation of the two cell types.

Table 2 Median CD8$^+$ T cells densities (number of cells/mm^2) of HIV$^+$ and HIV$^-$ patients. The results of the exact (permutation) Wilcoxon sign rank tests are shown in brackets

Sample	*Sero status*	*N*	*All CD8*		*Parenchymal*		*Perivascular*	
Autopsies	PML+							
	HIV$^-$	9	18.6	$P = 0.77$				
	HIV+	21	18.9					
	Total	30	18.7	$P = 0.0006$	16.2	$P = 0.0004$	3.3	$P = 0.04$
	PML$^-$							
	Total	5	1.6		0.09		1.3	
Biopsies	PML+			$P = 0.02$				
	HIV$^-$	11	28.1	$P = 0.06$				
	HIV+	5	111.6					
	Total	16	35.2					

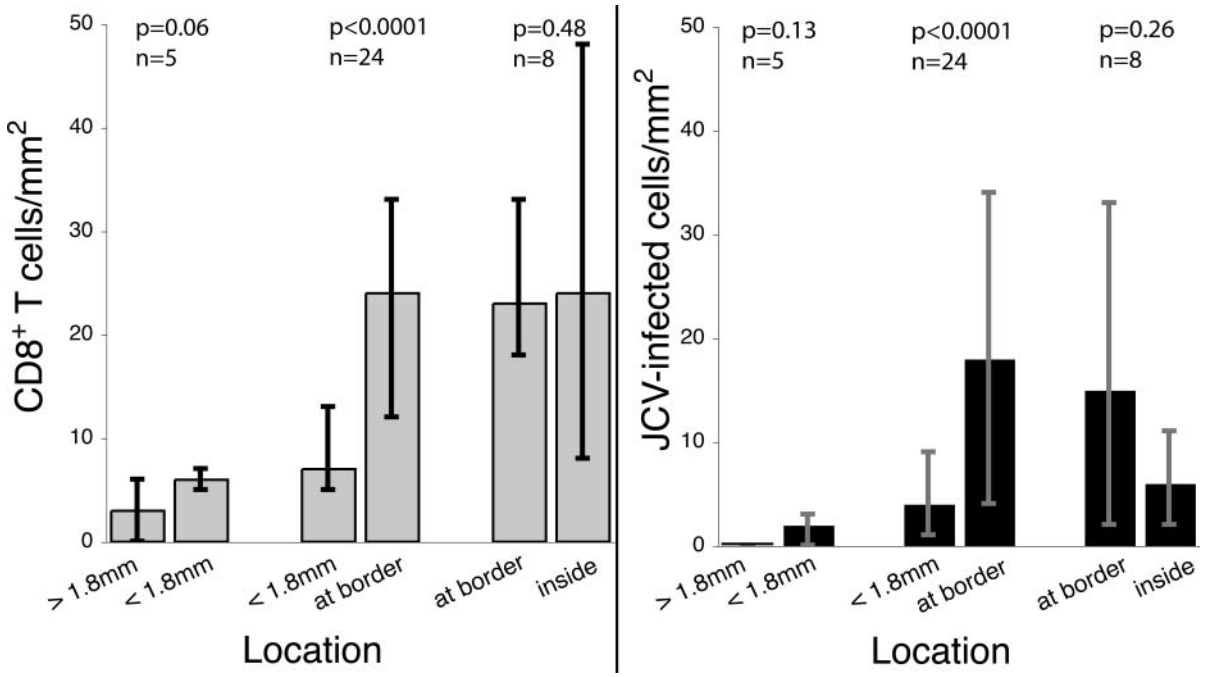

Figure 4 Densities (number of cells/mm^2) of CD8$^+$ T cells (panel A) and JCV-infected cells (panel B) at various locations. Statistical comparisons of cells frequencies were done by pairs of location (>1.8 mm versus <1.8 mm away from lesion, <1.8 mm versus at the border of the lesion, at the border versus inside of the lesion). Only patients who had at least 20 squares in each location under comparison were included in the tests. The results (p) and the number of patients (n) available for each Wilcoxon sign rank statistical test are indicated. Error bar: interquartile range (IQR).

Overall HIV$^+$ cases did not differ significantly from HIV$^-$ cases in Spearman rank correlations or model results. Representative examples of CD8$^+$ T cells surrounding JCV-infected cells are shown in Figure 5.

Discussion

It is known that T lymphocytes play a crucial role in the immune control of viral infections, but their distribution in PML lesions has not been precisely examined. Our qualitative studies indicate that CD8$^+$ T cells are the major lymphocyte type present in PML lesions of both HIV$^+$ and HIV$^-$ patients. In the latter group, this was the case even in CLL patients that had high numbers of CD20$^+$ B cells in perivascular cuffs but only a few in the parenchyma. These results are particularly significant since we have demonstrated that JCV-specific CTL are found in the blood and CSF of PML survivors (Du Pasquier *et al*, 2003; Koralnik *et al*, 2002; Du Pasquier *et al*, 2004), and since their early presence after disease onset is associated with control of PML (Du Pasquier *et al*, 2004). Because there is no specific treatment for JCV, medications aiming at increasing the cellular immune response against this virus may be instrumental in containing JCV replication and may improve the clinical outcome of patients with PML. However this type of therapy would only succeed if activated CD8$^+$ T cells are able to penetrate the CNS and destroy virus-infected glial cells.

Prior to embarking on such treatment studies, a prerequisite is to determine whether CD8$^+$ T cells can recognize JCV-infected cells in the brain, despite the high degree of immunosuppression of PML patients. Therefore, we explored the co-localization of CD8$^+$ T cells and JCV-infected cells in PML lesions, as an indirect estimation of antigen specificity of CD8$^+$ T cells. Our results show that in most PML patients, regardless of HIV serology status, CD8$^+$ T cells are topographically distributed around

Table 3 Summary of the Spearman correlations coefficients (CC) obtained for JCV-infected cells and all CD8$^+$ T cells, parenchymal and perivascular CD8$^+$ T cells, in autopsies and biopsies of HIV$^+$ and HIV$^-$ patients. In each case, the squares containing no JCV-infected cells and no CD8$^+$ T cells (0/0 squares) are omitted from the calculations. The level of significance (Sig) is 0.05 ($p < 0.05$).

Sample	*CC between JCV and CD8*	*Sero status*	*N*	*% Sig Pos CC*	*% Sig Neg CC*
Autopsies	All CD8	Total	30	77	10
		HIV+	21	76	10
		HIV$^-$	9	78	11
	Parenchymal CD8	Total	30	77	10
		HIV+	21	76	10
		HIV$^-$	9	78	11
	Perivascular CD8	Total	30	3	57
		HIV+	21	5	53
		HIV$^-$	9	0	67
Biopsies	All CD8	Total	16	25	0
		HIV+	5	0	0
		HIV$^-$	11	36	0

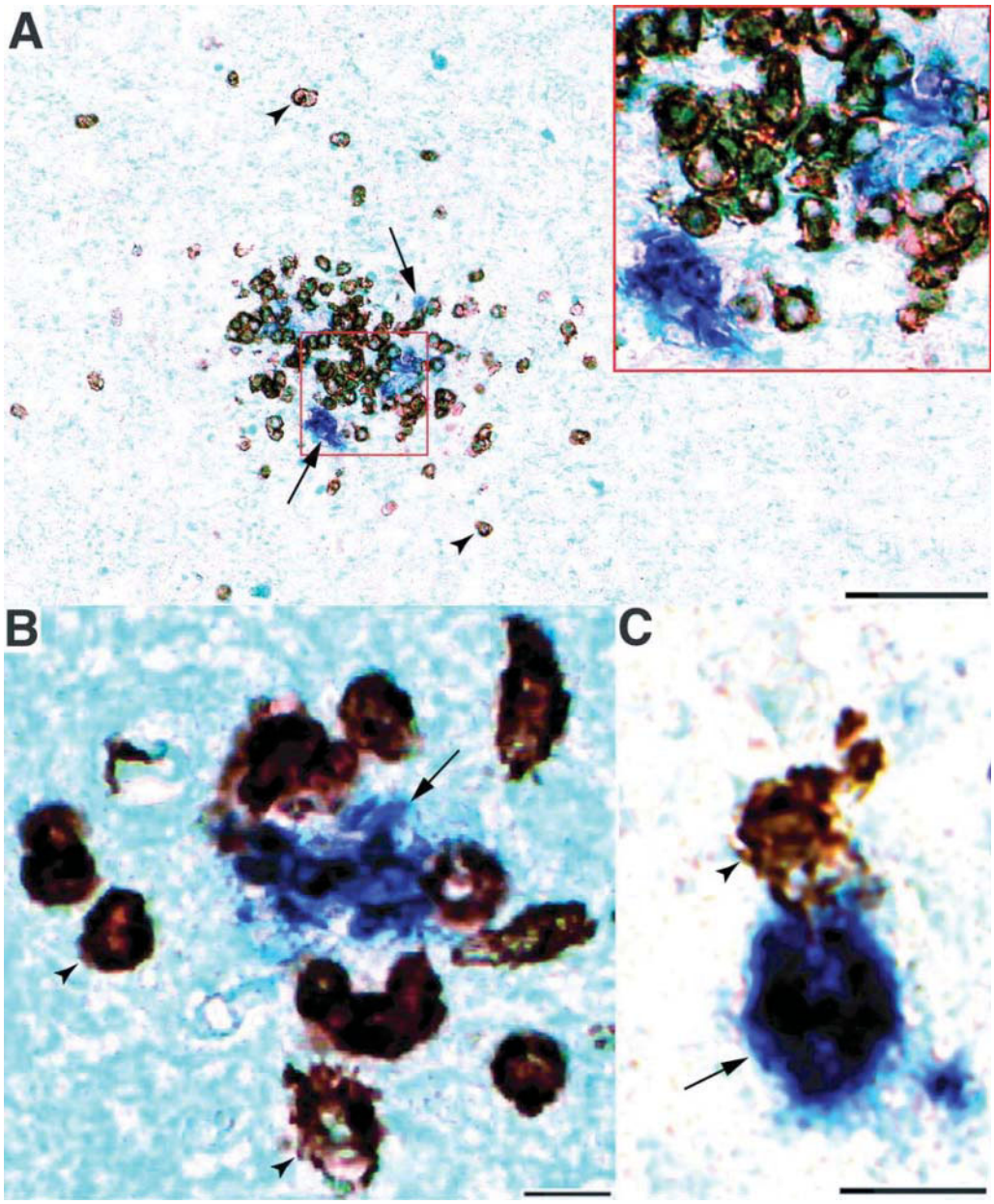

Figure 5 Close co-localization of CD8$^+$ T cells with JCV-infected cells can be observed in many HIV$^-$ (panels A, bar: 100 μm & C, bar: 10 μm) and HIV$^+$ individuals (panel B, bar: 10 μm). Double staining with anti CD8 and anti polyomavirus abs reveals numerous CD8$^+$ T cells (brown, arrowheads) aggregating around few JCV-infected cells (blue, arrows). Some CD8$^+$ T cells are in direct contact with JCV-infected cells (panel C). Such aggregates of CD8$^+$ T cells and JCV-infected cells can be found throughout the CNS white matter of PML patients.

JCV-infected cells in PML lesions, even when the effects of demyelination and location are removed, suggesting that CD8$^+$ T cells may be retained in the CNS in an antigen-specific fashion. Furthermore, the fact that the correlations between JCV-infected cells are mostly positive with CD8$^+$ T cells in the parenchyma and mostly negative with vessel-associated CD8$^+$ T cells is consistent with an active inflammatory process: the CD8$^+$ T cells remained in the vessels and/or perivascular cuffs when away from PML lesion, but spread into the parenchyma when within the proximity of JCV-infected cells. This would likely not be the case if CD8$^+$ T cells were not able to recognize JCV-infected cells or another associated factor, as one would expect that they would be either absent or randomly distributed in the brain tissue, with no significant correlation with JCV-infected cells.

In addition, our quantitative analysis indicates that the densities of both CD8$^+$ T cells and JCV-infected cells are the highest at the border of the PML lesions, while they get lower with increasing distance to the

lesions, and that these cells are rare or absent in the brain of healthy individuals. These results, and the fact that the co-localization of $CD8^+$ T cells and JCV-infected cells are still significant when the extent of demyelination and location are taken into account sheds a new light on the pathogenesis of this disease. It is known that PML lesions expand in a centrifugal fashion by cell to cell transmission of JCV, ultimately leaving demyelinated areas devoid of oligodendrocytes in the center, while infected glial cells are mainly located at the border of the lesions. Our data suggest that $CD8^+$ T cells are attracted to and accumulate in PML lesions and especially near JCV-infected cells. They may participate in the demyelinating process, possibly by destroying JCV-infected cells. Indeed, $CD8^+$ T cells remain in large numbers in the center of the lesions, especially in areas of high demyelination, and in many active lesions, these $CD8^+$ T cells are found on the lesion edge, suggesting that they are seemingly moving out with the active demyelinating process. Although both JCV itself and $CD8^+$ T cells could cause oligodendrocyte cell death, the consequences for the patient may be quite different. While a lytic infection of oligodendrocytes leads to production of large numbers of JC virions and viral propagation to nearby cells, the cytolytic activity of $CD8^+$ T cells on infected oligodendrocytes may occur early in the virus life cycle, before the assembly of mature viral particles, thereby preventing the spread of the disease in the CNS. Whether such mechanisms are operative *in vivo* were not determined in this study and we cannot rule out that, alternatively, $CD8^+$ T cells could be recruited in the PML lesions by chemokines produced by JCV-infected cells, irrespective of their specificity. It is also possible that the $CD8^+$ T cells within the lesions are unable to kill JCV-infected cells, even if they are attracted by these cells and are perhaps able to recognize them. Indeed, their presence in many of the samples tested did not prevent progression of the disease to death. Proper function of $CD8^+$ T cells may be dependent on $CD4^+$ T cells, which are typically depleted in the blood of immunosuppressed individuals who develop PML, and which were absent or rare as well in the brain parenchyma of all our patients.

There are several limitations to this study. Because PML is a rare disease, we used archival samples collected in several institutions over more than four decades. HAART has been shown to improve survival in PML (Antinori *et al*, 2003). Of 26 HIV^+ patients with PML, only 3 had been treated with HAART, since most samples had been collected before 1996. Therefore, the effect of HAART on the co-localization of $CD8^+$ T cells and JCV-infected cells could not be determined. For the same reason, our series does not contain any specimen of PML occurring in the context of immune-reconstitution inflammatory syndrome (IRIS) (Vendrely *et al*, 2005). Furthermore, the number of patients who survived more than one year or who had inactive disease at the time of histological diagnosis was very limited. Therefore, it is not possible to assess whether the frequency of $CD8^+$ T cells in PML lesions was correlated with a better clinical outcome.

In addition, whereas autopsy samples provide abundant material for analysis, they originate by definition from patients who succumbed to PML or to their underlying immunosuppression, and the frequency of $CD8^+$ T cells in such specimens may not be representative of the patient's immune response at the onset of PML. It is therefore remarkable to find a high percentage of positive correlations between $CD8^+$ T cells and JCV-infected cells in these autopsy samples, even when we removed the effects of location and demyelination with the Poisson regression model.

On the contrary, staining of $CD8^+$ T cells in biopsy samples is indicative of the early cellular immune response against JCV in the CNS. However, the amount of material available in biopsies is usually very small and the analysis is limited to a single time point. Nevertheless, we found that $CD8^+$ T cells co-localized with JCV-infected cells in the majority of these specimens. Thus, evidence from both situations represented by autopsy and biopsy suggests active, ongoing $CD8^+$ T cell responses that may be specific to JCV in the CNS.

Another pitfall in HIV^+ patients is the possible recruitment of $CD8^+$ T cells in response to other CNS pathogens, including HIV. This was ruled out by histological examination prior to the study, and by exclusion of cases with positive IHC for HIV p24 Ag. In HIV encephalopathy (HIVE) the distribution of HIV-infected macrophages is mainly perivascular, and $CD8^+$ T cells aggregating around HIV-infected cells are also distributed around the vessels (pers. observation). This perivascular distribution of $CD8^+$ T cells has been described in monkeys with simian immunodeficiency virus encephalopathy (Kim *et al*, 2004) and is different than the observations in our study.

Similarly, all HIV^- PML patients with leukemia who had autopsy material available for study had CLL, a proliferation of B lymphocytes, which were preferentially located in perivascular cuffs. Therefore the predominance of $CD8^+$ T cells in the parenchyma of these patients' PML lesions cannot be explained by their underlying malignancy.

Our findings underscore the importance of $CD8^+$ T cell immunosurveillance in the prevention of JCV reactivation. Indeed, two HIV^- patients with MS and one with Crohn's disease recently developed PML after treatment with natalizumab, a humanized monoclonal antibody binding to $\alpha 4$ integrins on the surface of lymphocytes, which prevents their normal penetration into the brain parenchyma and in other tissues (Berger and Koralnik, 2005; Drazen, 2005; Kleinschmidt-Demasters and Tyler, 2005; Langer-Gould *et al*, 2005; Van Assche *et al*, 2005). Post mortem analysis of the brain lesions of two of them

did not show any lymphocytic infiltrates while the brain biopsy of the patient who survived had only sparse lymphocytes. These data suggest that in these patients, there were sustained CD8$^+$ T cell-mediated responses against JCV in the periphery, which when interrupted resulted in the spread of the virus to the brain. Impaired immunosurveillance in the CNS may have then led to the emergence of PML.

Our study is also consistent with non-invasive studies of brain metabolism in PML lesions by proton magnetic resonance spectroscopy (^{1}H-MRS). Increased myoinositol (mI), a marker of CNS inflammation, was predictive of a better clinical outcome in PML patients (Katz-Brull *et al*, 2004). In addition, contrast enhancement of PML lesions on MRI, indicating local inflammation and breakdown of the blood-brain barrier, was also associated with long term survival (Berger *et al*, 1998). Based on our results, this inflammation may possibly be caused by active destruction of JCV-infected glial cells by CD8$^+$ T cells early after PML onset. Immunotherapy aimed at increasing this cellular immune response may well limit the extent of neurological damage caused by JCV in the CNS, while treatments limiting antiviral immunosurveillance may lead to the reactivation of JCV and the development of PML.

Material and methods

Origin of brain samples
Formalin-fixed, paraffin-embedded archival brain tissue samples from 46 patients with histologically confirmed PML were used in this study. These materials were collected from the departments of pathology of the Beth Israel Deaconess Medical Center, the Brigham and Women's Hospital, and the Massachusetts General Hospital in Boston, and the National NeuroAIDS Tissue Consortium (Morgello *et al*, 2001) between the years 1963 to 2004. The histological diagnosis of PML was established by a neuropathologist (JTJ, UDG, THW and members of the National NeuroAIDS Tissue consortium). All samples had: 1) positive detection of JCV antigen or DNA in our laboratory, 2) no evidence of HIV encephalitis (HIVE) demonstrated by absence of histological features of HIVE and HIV p24 Ag in samples from HIV$^+$ cases, 3) detection of at least 3 CD8$^+$ T cells by immunohistochemistry (IHC) and 4) detection of at least 3 JCV-infected glial cells by in situ hybridization (ISH) or by IHC in the selected tissue. Of 46 PML patients, 26 were HIV$^+$. The 20 HIV$^-$ patients with PML had the following underlying diseases: 6 CLL, 2 vascular disease (stroke), 1 chronic myelogenous leukemia (CML), 1 acute myelogenous leukemia (AML), 1 lymphoma, 1 malignant thymoma, 1 lung transplant recipient, 1 polymyositis and 6 patients whose predisposing disease was not available. Autopsy samples from 4 HIV$^+$ without HIVE and 1 HIV$^-$ patients without PML were used as controls and were included in the quantitative analyses with the PML cases. In addition, 3 HIV$^+$ patients with HIVE were qualitatively studied.

Clinical characteristics and PML disease classification
Detailed clinical histories were available on 44/46 cases through clinical or pathology records. (See Table 1 for the distribution of various patient and specimen characteristics overall and separately for autopsied and biopsied patients.) There were 21 HIV$^+$ and 9 HIV$^-$ autopsies and 5 HIV$^+$ and 11 HIV$^-$ biopsies. HIV$^-$ patients with PML tended to be older than the HIV$^+$ patients with PML (median 58 and range 36 to 79 vs. median 40 and range 30 to 53, $p < 0.0001$). The PML disease was considered active or inactive if clinical or radiological signs of disease progression were present or absent, respectively, at the time of the biopsy or autopsy. In 2 cases of PML the disease was discovered at autopsy only.

Immunohistochemistry (IHC)
Antibodies: The following primary Abs were used for this study. JCV-infected cells: Polyclonal Cytimune rabbit antiserum to SV40 (Lee Biomolecular, San Diego, CA, 1:1000), which cross-reacts with JCV. HIV-infected cells: Mouse anti HIV p24 (Dako, Carpinteria, CA, 1:10). Astrocytes: mouse anti-human GFAP (Dako, 1:50) or rabbit anti-cow GFAP (Dako, 1:2000). T lymphocytes: mouse anti-human CD8 (NCL-CD8-295-1A5, Novocastra, Newcastle-upon-Tyne, UK, 1:50), mouse anti-human CD4 (NCL-L-CD4-1F6, Novocastra, 1:20), mouse anti-human CD4 (clone 1F6, NeoMarkers, Fremont, CA), mouse anti-human CD3 (NCL-L-CD3-PS1, Novocastra, 1:100). B lymphocytes: mouse anti-human CD20cy, (Dako, 1:100).

Single and double label IHC: All tissue sections were deparaffinized for two hours at 57°C. The sections used for staining with anti CD4, CD8 or SV40 Abs were then treated in an electric pressure cooker for 15 min in Trilogy solution (Cell Marque, Hot Springs, AR) for deparaffinization, rehydration and antigen retrieval as previously described (Kim *et al*, 2004). Sections used for staining with anti CD3 and CD20 alone were deparaffinized in xylene and rehydrated through graded alcohols to PBS. Rehydrated sections were then heated in microwave oven at 800 W for 20 minutes with antigen unmasking solution (Vector, Burlingame, CA) and cooled for 20 minutes at room temperature. For all wash steps, phosphate-buffered saline (PBS) was used. The Envision double stain kit (Dako) was used according to the manufacturer's instructions except that longer incubation times (30-60 minutes) were used for secondary Abs (alkaline phosphatase and horseradish peroxidase (HRP) labeled polymers). A protein block (Dako) was used for 30 minutes before incubation with the primary Abs.

Negative controls for IHC comprised omission of the primary Abs and use of sections from healthy patients. For the positive controls, we used sections of HIV$^-$ and HIV$^+$ PML patients (JCV), HIV$^+$ patients with HIVE (p24 Ag) and tonsil sections from healthy individuals (CD20, CD4 and CD8). The chromogenic substrates used for alkaline phosphatase were NBT/BCIP (Roche, Indianapolis, IN) or Vector® Blue (Vector, Burlingame, CA). For HRP, the chromogens were 3,3'-diaminobenzidine tetrahydrochloride (Dako), Vector® NovaRed and Vector® VPI (Vector, Burlingame, CA). For HRP chromogen, endogenous peroxidase blocking solution (Dako) was applied during 3 minutes before the protein block, except for the CD4, where it was applied before the Trilogy pretreatment. Sections were then lightly counterstained with luxol fast blue (LFB) stain for myelin.

Double stainings of JCV-infected cells and CD8$^+$ T cells done specifically for image analyses: Since preliminary qualitative observations showed that only CD8$^+$ T cells and JCV-infected cells were significantly present in the PML samples, quantification by image analysis was performed only on slides which were double-stained for JCV-infected cells and CD8$^+$ T cells (IHC). When the viral DNA was well preserved (61% of the cases), the detection of JCV-infected cells was done by ISH while in old archival cases with low DNA preservation, IHC was performed. The results of both type JCV detection used in the double stainings were combined after statistical analyses showed that the type of detection of JCV-infected cells had no influence on the final results. For simultaneous detection of virus nucleic acid and CD8$^+$ T cells in the same tissue section, ISH for JCV DNA was followed with IHC against CD8 as previously described (Kim *et al*, 2004). In this technique, the combination of the two heat-induced epitope-retrieval methods, pressure cooker and microwave, was used to achieve CD8 antigen retrieval from paraffin-embedded tissues and to improve ISH of viral nucleic acid. Briefly, after incubation in an oven for 2 hrs at 60°C, tissue sections were deparaffinized and rehydrated in an electric pressure cooker in Trilogy solution (Cell Marque, Hot Springs, AR) for 15 min. The sections were then subjected to microwave pretreatment with antigen unmasking solution (Vector Laboratories), washed with PBS for 5 min, and immersed in PBS containing 0.15% Triton X-100 for 10 min at room temperature. Sections were rinsed twice for 10 min each in 2x saline-sodium citrate buffer (SSC). Before hybridization, 200 ml of prehybridization buffer containing 10% dextran sulfate, 4x SSC, 2mM EDTA, 50% deionized formamide, 1x Denhardt's solution, 500 mg/ml herring sperm DNA, and 500 mg/ml yeast tRNA (all reagents from Sigma, St. Louis, MO) were applied to sections. After incubation for 1 h at 45°C, hybridization mixtures containing 1 mg/ml biotinylated JCV DNA probes (Enzo Diagnostics, Farmingdale, NY) were applied to the sections, and hybridized at 45°C overnight. The sections were subjected to two 15' washes at 45°C in 2x SSC, 1x SSC, and 0.1x SSC, and then washed in buffer 1 (100 mM Tris-HCl and 150 mM NaCl, pH 7.6) for 5 min. After pre-incubation of sections for 30 min at room temperature with Buffer 1 containing 1% blocking reagent (Roche, Indianapolis, IN), the sections were incubated with 1:1000 dilution of alkaline phosphatase conjugated streptavidin for JCV DNA probe for 2 h at room temperature. The sections were washed in buffer 1 twice for 10' each, and rinsed in buffer 2 (100 mM Tris-HCl, 100 mM NaCl, and 50 mM $MgCl_2$, pH 9.5) for 5'. Hybridized probes were detected using 5-bromo-4-chloro-indolylphosphate/nitroblue tetrazolium (NBT/BCIP; Roche) as the chromogen substrate. Sections were rinsed with 1x PBS before immunostaining. Negative controls included non-infected tissues and omission of the DNA probe. After ISH, IHC against CD8 was performed as described above. Sections were then lightly counterstained with LFB stain for myelin. Slides were coverslipped with Eukitt Mounting Medium (Electron Microscopic Sciences, Washington, PA).

When the detection of JCV-infected cells in the double stainings had to be done by IHC, the protocol described in the precedent chapter was used with the difference that we applied the same antigen retrieval treatment that the one which was done for the combined ISH against JCV and IHC against CD8$^+$ T cells described in this article.

Quantitative image analysis

Images: For each of the slides which were double stained for JCV-infected cells and CD8$^+$ T cells, up to 500 contiguous, non-compressed 1280 × 960 pixels TIFF images encompassing the entire sample (biopsies) or from 1–2 cm^2 of a representative area (autopsies) were acquired with a DFW-SX900 Sony Firewire color camera and with the shareware BTV 5.2 (www.bensoftware.com). The camera was mounted on an Olympus BX40 light microscope and connected to an Apple PowerBook G4. A magnification of 10x (optic) was chosen so that it was possible to differentiate and individualize the JCV-infected cells and the CD8$^+$ T cells. The images were spatially calibrated with the freeware Image J 1.28v (http://rsb.info.nih.gov/ij/) on the basis of a micrometric slide picture acquired in the same conditions. Thus, it was determined that 1 pixel on the acquired images corresponded to a real distance of 0.844 μm. The contiguous images of each biopsy and autopsy were then merged with the plug-in Automatch (Photoshop CS).

Cell counting: To quantify JCV-infected cells and CD8$^+$ T cells in large tissue sections requires both high resolution images where the phenotype of the

cells can be easily recognized and low power views to encompass large lesions. To reconcile these mutually exclusive requirements, we made high-resolution montages to localize JCV-infected cells, CD8$^+$ T cells and areas of demyelination. In the case of the autopsies, an adjacent tissue section was stained with LFB and H&E and scanned at a resolution of 1200 dpi to show the distributions of the anatomical landmarks (gray and white matter) as well as the demyelinated areas. This high-contrast, low-resolution image, was then scaled, rotated and superimposed on the high-resolution image (montage) of the JCV-infected and CD8$^+$ T cells. A third layer representing a 600 by 600 μm (711 pixels) square grid was then added randomly to the resulting image. The final image corresponded to a Photoshop file comprising a first layer with the architecture of the tissues, a second layer showing the distribution of JCV-infected and CD8$^+$ T cells and a third layer with the 600 $\times$ 600 μm grid, from which data was analyzed. In autopsies, only grid squares completely filled with tissue were used for cell counting. In biopsies, partial squares (at the edge of the tissue) were also used for cell counting, and the tissue area in each square was recorded. The total number of grid squares examined for the autopsies ranged from 148 to 378, with a median of 252 (corresponding to a tissue area of 90 mm^2). The total number of grid squares examined for the biopsies ranged from 2 to 232, with a median of 11 (4 mm^2), and only 2 of the 16 cases had more than 20 grid squares examined.

Each grid square was classified relative to the demyelinated lesions, which were present either in the white matter or at the junction between the grey and white matter. Those squares that were entirely contained in an area of demyelination were defined as "inside," the squares that did not contain any demyelination were defined as "outside," and those that included both non demyelinated and demyelinated tissues were considered to be at the 'border' of the area of demyelination. To study the effect of the distance from the lesion on the distribution of the CD8$^+$ T cells in the squares which were outside, the squares were classified as ">1.8 mm" (from all lesions) when the nearest sign of infection (demyelination or JCV-infected cell) was more than 3 squares (1.8 mm) away from the square under consideration, or as "<1.8 mm" in the other cases.

In the autopsies, the number of JCV-infected cells, the number of CD8$^+$ T cells associated with the CNS vessels (inside the vessel wall or in contact with perivascular cuffs), the number of CD8$^+$ T cells present in the brain parenchyma, and finally the total number of CD8$^+$ T cells were determined. For biopsies, which were usually devoid of large vessels, the total number of CD8$^+$ T cells only, was determined. The cells were counted in each square of the montage, which was displayed at high magnification on the computer's screen.

The cell densities of each square, defined as number of cells/mm^2, were then calculated. Finally, the extent of demyelination in each of the squares was evaluated using the following scale: no or low demyelination (0–50%) or high (51–100%) demyelination with tissue degradation.

Statistical analysis: The exact (permutation) Wilcoxon sign rank test was used to compare paired values (e.g., correlations of JCV-infected cells and parenchymatous vs. perivascular CD8$^+$ T cells) and the exact (permutation) Wilcoxon rank sum test was used to compare two unmatched groups (e.g., results in HIV$^-$ and HIV$^-$ patients) (Wilcoxon, 1945).

We used the Spearman rank correlation coefficient (equivalent to Pearson's correlation coefficient calculated on ranks) to study the topographic association between CD8$^+$ T cells and JCV-infected cells; the test of whether the correlation coefficient was significantly different from zero used the same (Fisher) transformation as is used with the Pearson correlation. This method was chosen to minimize the effect of outliers and to produce robust results even in non-gaussian distributions. In both biopsy and autopsy materials, some of the grid squares examined lacked both CD8$^+$ T cells and JCV-infected cells (0/0 squares). The number of such squares could have large effect on the correlation between CD8$^+$ T cells and JCV-infected cells, and would be expected to artificially increase positive correlations and make them more significant; they could also make negative correlations less significant. In addition, the biopsy specimens had fewer 0/0 squares than the autopsy specimens. Therefore, we decided to omit the 0/0 squares from the analyses.

Linear regression (ordinary least squares) was used to examine the effect of patient and specimen characteristics on Spearman correlation coefficients. Poisson regression was used to examine the effect of grid square characteristics (and also the effect of densities of JCV cells) on densities of CD8$^+$ T cells.

References

Aksamit AJ, Gendelman HE, Orenstein JM, Pezeshkpour GH (1990). AIDS-associated progressive multifocal leukoencephalopathy (PML): comparison to non-AIDS PML with in situ hybridization and immunohistochemistry. *Neurology* **40:** 1073–1078.

Antinori A, Cingolani A, Lorenzini P, Giancola ML, Uccella I, Bossolasco S, Grisetti S, Moretti F, Vigo B, Bongiovanni M, Del Grosso B, Arcidiacono MI, Fibbia GC, Mena M, Finazzi MG, Guaraldi G, Ammassari A, d'Arminio Monforte A, Cinque P, De Luca A (2003). Clinical

epidemiology and survival of progressive multifocal leukoencephalopathy in the era of highly active antiretroviral therapy: data from the Italian Registry Investigative Neuro AIDS (IRINA). *J Neurovirol* **9 (Suppl 1):** 47–53.

Astrom KE, Mancall EL, Richardson EP (1958). Progressive multifocal leukoencephalopathy. *Brain* **81:** 93–127.

Berger JR, Koralnik IJ (2005). Progressive Multifocal Leukoencephalopathy and Natalizumab—Unforeseen Consequences. *N Engl J Med* **353:** 414–416.

Berger JR, Levy RM, Flomenhoft D, Dobbs M (1998). Predictive factors for prolonged survival in acquired immunodeficiency syndrome-associated progressive multifocal leukoencephalopathy. *Ann Neurol* **44:** 341–349.

Drazen JM (2005). Patients at Risk. *N Engl J Med* **353:** 417.

Du Pasquier RA, Kuroda MJ, Schmitz JE, Zheng Y, Martin K, Peyerl FW, Lifton M, Gorgone D, Autissier P, Letvin NL, Koralnik IJ (2003). Low frequency of cytotoxic T lymphocytes against the novel HLA-A*0201-restricted JC virus epitope VP1(p36) in patients with proven or possible progressive multifocal leukoencephalopathy. *J Virol* **77:** 11918–11926.

Du Pasquier RA, Kuroda MJ, Zheng Y, Jean-Jacques J, Letvin NL, Koralnik IJ (2004). A prospective study demonstrates an association between JC virus-specific cytotoxic T lymphocytes and the early control of progressive multifocal leukoencephalopathy. *Brain* **127:** 1970–1978.

Katz-Brull R, Lenkinski RE, Du Pasquier RA, Koralnik IJ (2004). Elevation of myoinositol is associated with disease containment in progressive multifocal leukoencephalopathy. *Neurology* **63:** 897–900.

Kim WK, Corey S, Chesney G, Knight H, Klumpp S, Wuthrich C, Letvin N, Koralnik I, Lackner A, Veasey R, Williams K (2004). Identification of T lymphocytes in simian immunodeficiency virus encephalitis: Distribution of CD8+ T cells in association with central nervous system vessels and virus. *J Neurovirol* **10:** 315–325.

Kleinschmidt-Demasters BK, Tyler KL (2005). Progressive Multifocal Leukoencephalopathy Complicating Treatment with Natalizumab and Interferon Beta-1a for Multiple Sclerosis. *N Engl J Med* **353:** 369–374.

Koralnik IJ, Du Pasquier RA, Kuroda MJ, Schmitz JE, Dang X, Zheng Y, Lifton M, Letvin NL (2002). Association of prolonged survival in HLA-A2+ progressive multifocal leukoencephalopathy patients with a CTL response specific for a commonly recognized JC virus epitope. *J Immunol* **168:** 499–504.

Koralnik IJ, Du Pasquier RA, Letvin NL (2001). JC virus-specific cytotoxic T lymphocytes in individuals with progressive multifocal leukoencephalopathy. *J Virol* **75:** 3483–3487.

Koralnik IJ, Schellingerhout D, Frosch MP (2004). Case records of the Massachusetts General Hospital. Weekly clinicopathological exercises. Case 14-2004. A 66-year-old man with progressive neurologic deficits. *N Engl J Med* **350:** 1882–1893.

Langer-Gould A, Atlas SW, Bollen AW, Pelletier D (2005). Progressive Multifocal Leukoencephalopathy in a Patient Treated with Natalizumab. *N Engl J Med* **353:** 375–381.

Morgello S, Gelman BB, Kozlowski PB, Vinters HV, Masliah E, Cornford M, Cavert W, Marra C, Grant I, Singer EJ (2001). The National NeuroAIDS Tissue Consortium: a new paradigm in brain banking with an emphasis on infectious disease. *Neuropathol Appl Neurobiol* **27:** 326–335.

Padgett BL, Walker DL, ZuRhein GM, Eckroade RJ, Dessel BH (1971). Cultivation of papova-like virus from human brain with progressive multifocal leucoencephalopathy. *Lancet* **1:** 1257–1260.

Richardson EP, Jr., Johnson PC (1975). Atypical progressive multifocal leukoencephalopathy with plasma-cell infiltrates. *Acta Neuropathol Suppl (Berl)* **Suppl:** 247–250.

Van Assche G, Van Ranst M, Sciot R, Dubois B, Vermeire S, Noman M, Verbeeck J, Geboes K, Robberecht W, Rutgeerts P (2005). Progressive Multifocal Leukoencephalopathy after Natalizumab Therapy for Crohn's Disease. *N Engl J Med* **353:** 362–368.

Vendrely A, Bienvenu B, Gasnault J, Thiebault JB, Salmon D, Gray F (2005). Fulminant inflammatory leukoencephalopathy associated with HAART-induced immune restoration in AIDS-related progressive multifocal leukoencephalopathy. *Acta Neuropathol (Berl)* **109:** 449–455.

Wilcoxon F (1945). Individual comparisons by ranking methods. *Biometrics* **1:** 80–83.